Environmental Earth Sciences (2024) 83:139
https://doi.org/10.1007/s12665-023-11360-w

ORIGINAL ARTICLE

Wind and sand environment and spatial differentiation of sediment in the west desert of Yinshan Mountain in China

Xiya Liu[1] · Haibing Wang[1] · Hejun Zuo[1] · Nana Liu[2]

Received: 26 March 2023 / Accepted: 2 December 2023 / Published online: 21 February 2024

Abstract

To investigate the regular patterns by wind and sand in low hilly basins, we analyzed the particle size, component end element and fractal variability of surface sediments, as well as the near-surface wind energy and sand transport potential, and determined the characteristics of their spatial differentiation in the desert west of Yinshan Mountain in China. The results showed that the regional dominant wind was mainly westerly and southwest wind, and the average annual average wind speed of sand wind was 6.56–7.62 m s^{-1}, the annual average drift potential of the sand wind was 359.99 VU, and the average annual value of synthetic drift potential was 204.46 VU, which classified region as a the middle-wind-energy environment with middle-wind-direction variability. Under the action of dominant wind, the particle size of dune sediment gradually refined from the northwest to the southeast and northeast, and the fractal dimension gradually increased. The sediments of Baiyinchagan Desert, Boketai Desert, and southern Yamaleike Desert dunes were fine (the average particle size was 0.191 mm), and the average fractal dimension value was 2.372; the Haili Desert and the northern Yamaleike Desert dunes was large (the average particle size was 0.212 mm), and the average fractal dimension was 2.327. At the same time, fed by the near source Gobi coarse sand, under the action of long-term wind and sand, the Haili and Yamaleike Deserts formed tall and stable crescent sand dunes and sand dune chains. The particle size end member indicated that the desert sediment was wind deposit, while the desert peripheral Gobi desert end member indicated that the type of sediment was wind deposit and river alluvial material formed under the combined action of wind and water, the heterogeneity of the Gobi outside the desert was significantly higher than the desert surface, which showed moderate spatial differentiation. The topography of low mountains and hilly basins affected near-surface sandstorm processes and the formation and evolution of sandstorm landforms.

Keywords Sediment · Granularity · Wind and sand environment · Spatial specificity · The desert west of Yinshan Mountain

Introduction

Wind is an important force for shaping geomorphological forms in arid and semi-arid areas, and it is also a direct driving force of wind and sand damage (El-Baz and Hassan 1986; Dong et al. 2020). An accurate understanding of regional wind conditions and wind-energy environmental changes is necessary to understand the formation of global sandstorm activities. Gobi desert in Southern Mongolia–northwest China, Badain Jaran–Tengger–Ulan Buh Desert as the main body of the Asian dust source area (Zhang et al. 2019), Dust of Gobi desert in southern Mongolia–northwest China is easy to be strong westerly current long distance handling, among the dust of Gobi desert in spring, summer, 35% and 31%, respectively, were sent to east Asia (Chen et al. 2017). The west desert of Yinshan Mountain is located in the west of Lang Mountain and the south of the Altai Mountains. It is distributed in a hilly basin desert in the east of the Alxa Plateau, which is second in area only to the Badain Jaran and Tengger Deserts. It mainly includes four sand belts: Baiyinchagan, Haili, Boketai, and Yamaleike Desert (Zhu et al. 1974). The etable sand from the desert west of Yinshan Mountain and the Gobi desert

✉ Hejun Zuo
zuohj@126.com

[1] Inner Mongolia Key Laboratory of Aeolian Sand Physics and Sand Control Engineering, College of Desert Control Science and Engineering, Inner Mongolia Agricultural University, 29 Erdos East Street, Hohhot 010018, Inner Mongolia Autonomous Region, People's Republic of China

[2] Forestry and Grassland Development Center, Ordos City 017010, Inner Mongolia Autonomous Region, People's Republic of China

is transported to the Hetao Plain under the action of strong northwest wind, and part of the sand is deposited on the Gobi desert at the eastern foot of the Lang Mountain, which reduces the dust directly entering the Hetao oasis to a certain extent. The original sediments of Gobi desert surface are mixed with dune fields, which makes the grain size of surface sediments has obvious spatial differentiation, and indicates the effect of regional sand clearly (Shen et al. 2020).

The composition and type of wind and sand deposits of the dunes in west desert of Yinshan Mountains desert are significantly different. Some studies in the desert area have found strong wind activities, frequent dust events, a fast the desert expansion rate, and desertification developing rapidly. For example, the Haili Desert moves 3.23 m/a southeast every year, the western Boketai Desert moves 3.03 m/a east and southeast, and the entire desertified area west of Yinshan Mountain has increased by 24.65 km^2 over the past 30 years (Su 2020). In recent years, most researchers from the wind characteristics, surface sediment size, sand activity intensity of desert and surrounding aeolian environment conducted many studies, revealed the desert environment characteristics, mainly concentrated in the Xinjiang and Inner Mongolia area, such as Taklimakan Desert, Badain Jaran Desert, Gurbantunggut Desert, Tengger Desert, the Qaidam Basin Desert, and Ulan Buh Desert, etc. (Zhang et al. 2012; Wang et al. 2015; Li et al. 2021, 2022). Currently, because of the lack of systematic research, as well as the lack of long-term wind-energy environmental monitoring data, of the regional sand landform sediment characteristics, source environment, and wind and landform evolution, a comprehensive understanding of the evolution of the Alxa Plateau sand landform has been relatively insufficient.

Particle size is often used in the field of environmental geoscience as a theoretical method to reflect the morphology and characteristics of soil surface material (Udden 1898). It holds great significance in identifying the source background of sediment, identifying the sedimentary environment and reflecting the evolution of the paleoclimate (Zhou et al. 2021; Zhao et al. 2019; Porter and An 1995; Adam et al. 2009). Particle size distribution is an important surface characteristic parameter in the current global and regional scale dust cycle model. The study of sand dynamics shows that the sediment particle size composition is closely related to the wind energy acting on the surface, with the dynamic linkage changes of wind energy. The different distribution forms of surface sediments significantly affect the effective momentum transmission rate and dust supply capacity of the surface wind energy (Young and Sung 2010; Wang et al. 2021; Kermani and Boutiba 2023). Therefore, topsoil characteristic parameters can be defined according to the probability density function of particle size distribution, and reflect the characteristics of sediments and release potential of dust in aeolian surface (Wang et al. 2021; Li et al. 2017; Hossein et al. 2015).The particle size end element analysis method (Weltje 1997; Paterson and Heslop 2015) is able to use the particle size data more effectively to separate the content and multiple values of each component from the multi-component mixture, and can further analyze the sedimentation dynamic process corresponding to the particle size component..

In the 1970s, French mathematician Mandelbrot proposed the concept of a "fractal" (Mandelbrodt 1998). This natural phenomenon can be described by a "fractal dimension", which not only represents the morphological structure of soil particles and physical and chemical characteristics (San José Martínez et al. 2010; Xu et al. 2021) but also quantifies the characteristics of soil evolution on a certain spatial and temporal scale (Lu et al. 2018). The combination of sediment particle size and fractal model can be used to effectively identify the differences in sediment particles and also can make up for the limitations of using a single model. In addition, this combination well represents the spatial differentiation of surface sediments in arid areas (Liu et al. 2022; Mohammadi et al. 2019).

Therefore, we collected surface sediment samples from the west desert of Yinshan Mountain (Baiyinchagan, Haili, Boketai, and Yamaleike Deserts) and the surrounding Gobi desert. We conducted an analysis of the wind energy environment characteristics and particle size and its end member features, to explore the regularity of sediment spatial differentiation, to determine the sand deposition environment and regional sand landform formation process.

Materials and methods

Regional setting

The west desert of Yinshan Mountain is located in the northeast part of Alxa Plateau and the western part of Bayannur Plateau. It is distributed in the northwest of Lang Mountain, along the Mongolian Mountain flood fan edge, and north to the border of Mongolia. Administratively, it belongs to the Inner Mongolia Bayannur City Urat back flag, Inner Mongolia, geographic coordinates 39°41′22"N–42°17′14" N, 104° 16′24"E–106°59′14″E. The total desert area of this area is 7340.63 km^2, among which the Yamaleike Desert has the largest area, totaling 5600 km^2. Fixed dunes are mainly distributed in the northwest and desert edge zones, while semifixed dunes and mobile dunes are distributed in the vast valleys and basins of this area, with a height of 3–30 m and the highest height of 50 m. Most dune types are mainly crescent-shaped dune chains (Table 1). The four sand belts in the study area (Baiyinchagan, Boketai, Haili, and Yamaleike Deserts dunes) are not contiguous, but they are distributed

between the Gobi desert, presenting two distinct desert landscapes of desert dunes and Gobi desert (Figs. 1 and 2). The region is characterized by long-term drought and little rain, average annual precipitation < 100 mm, dryness $K > 5.0$, sparse vegetation, strong sand erosion, and 40–50 gale days per year. In long-term wind erosion and seasonal flooding, the area of the dunes and the Gobi desert, its arrangement structure, developmental age and stage, and landform differences create differences in the spatial distribution of the surface sediment. In the process of strong sand activities, the dunes–Gobi desert material supply and its internal dust cycle have created obvious spatial differentiation among the sediment features.

Research method

Sample collection and measurement

To explore the spatial differentiation of surface sediments in the west desert of Yinshan Mountain and the surrounding Gobi desert area, in the study area, we selected the surface with flat terrain, bare surface, and significant component differences. We collected a total of 259 sediment samples from 20 cm × 20 cm × 2 cm sand depth, which we loaded into a self-sealing bag. We collected 98 dune fields samples, including 11 from Baiyinchagan Desert, 21 from Haili Desert, 35 from Boketai Desert, and 31 from Yamaleike Desert; and collected 161 Gobi desert sample, including 48 from Baiyinchagan Gobi, 20 from Haili Gobi, 71 from Boketai Gobi, and 22 from Yamaleike Gobi.

In the laboratory, 200 g of each samples were dried and ground, and < 0.063 mm samples were tested using a Laser particle size meter. In this paper, 21 particle sizes were categorized according to the international soil texture grading standard, with a minimum size 0.05 mm to a maximum size 32 mm.

Particle size calculation and its end-element analysis

Particle size data and parameter characteristics reflect the sedimentary environment and genetic analysis of the sediment. In this study, we calculated sediment particle size parameters according to Folk and Ward (mean grain size M_Z, sorting

Table 1 Characteristics of the desert west of Yinshan Mountain

Region	Location	Area	Dune type
Baiyinchagan Desert	Northwest Wolf Mountain	1100 km^2	Fixed and semifixed sand ridges, the height of the dune is 10–20 m
Haili Desert	Northwest part of the Urat Back Banner	1260 km^2	Crescent sand dune chains, the height of the dune is 5–10 m or 20–40 m
Boketai Desert	North of the Urat Back Banner	3400 km^2	Crescent sand dune chains, lattice sand dunes, the height of the dune is 10–30 m
Yamaleike Desert	The northeast part of the Alxa Plateau	5600 km^2	Crescent sand dune chains, ridge dunes, dunes can reach up to 50 m

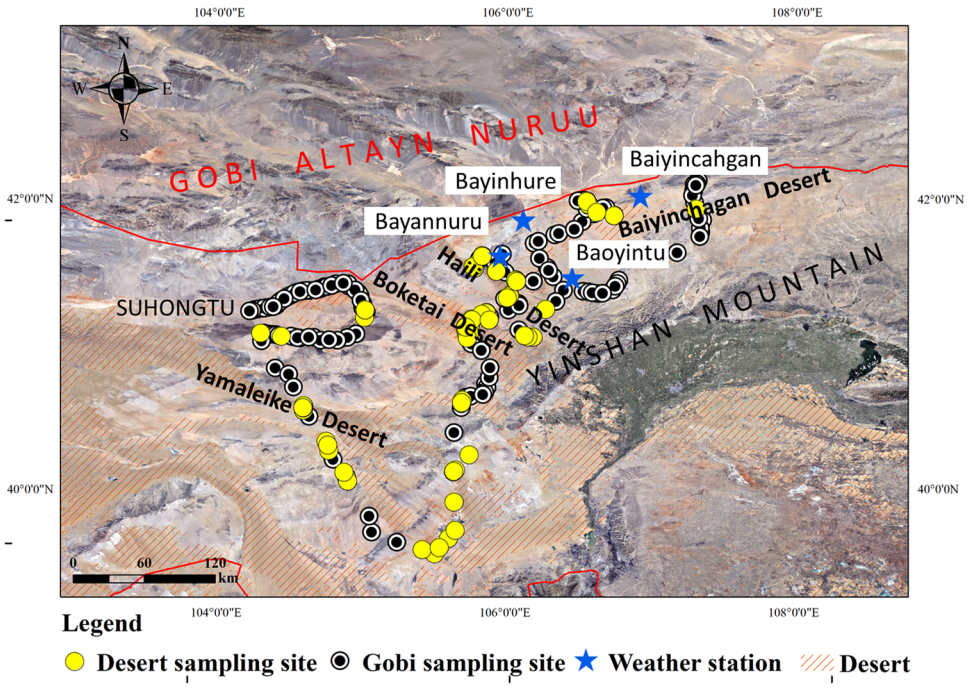

Fig. 1 Research area

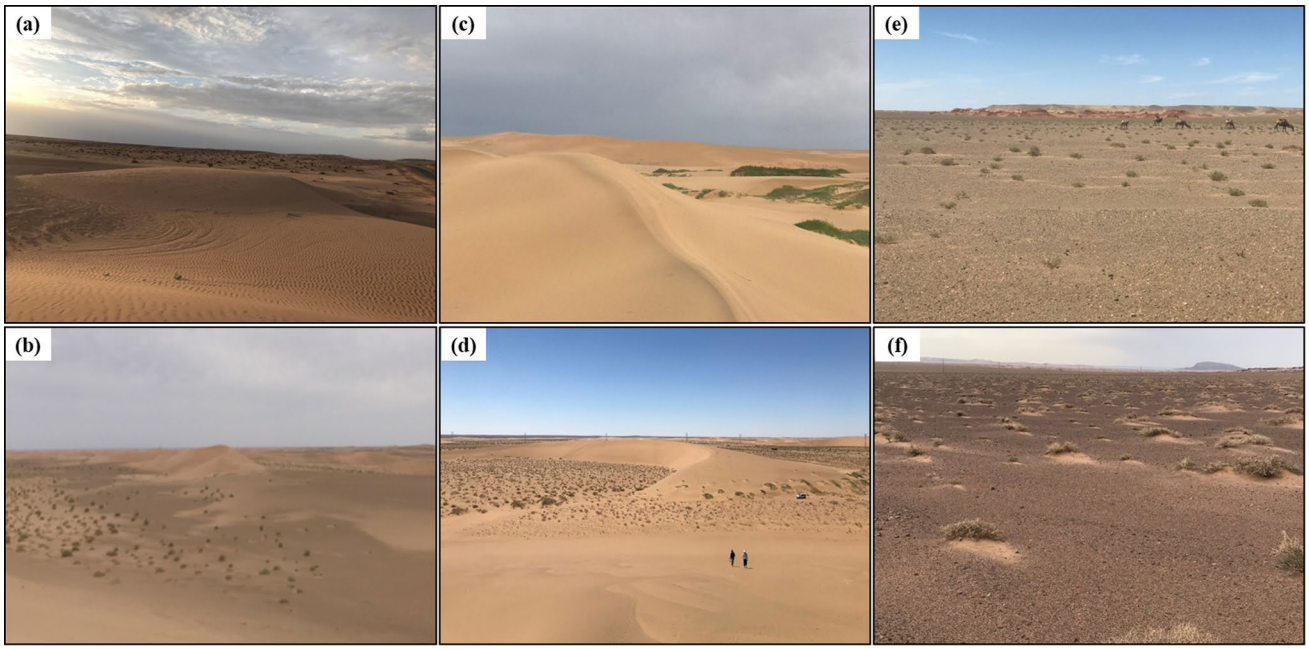

Fig. 2 Typical ground surface of the study area: **a** Baiyinchagan Desert, **b** Haili Desert, **c** Boketai Desert, **d** Yamaleike Desert, and **e**, **f** Gobi

value σ, skewness S_K, and kurtosis K_G) (Folk and Ward 1957). According to this analysis of the sediment particle spectrum change and the release potential of wind erosion dust, the Gobi surface sediment particles had three components, namely, (Wang et al. 2015; Nicholas and Craig 2011; Bullard et al. 2011), the wind erosion residual coarse sand and gravel components that do not participate in sandstorm activities, close distance transport wind erosion deposition components, and long distance dust release components. The critical particle size value of each component is closely related to the wind energy acting on the surface, and changes dynamically with the wind energy. The dust release component (E_p), wind erosion deposition component (D_p) and wind erosion residual component (R_p) are calculated in the particle spectrum change map (Fig. 3). The formula is as follows:

$$E_p = \text{The cumulative percentage of the Gobi on point A(\%)} - \text{The cumulative percentage of the Deserton point A(\%)} \quad (1)$$

$$R_p = ((1 - \text{The cumulative percentage of the Gobi on point B(\%)}) - (1 - \text{The cumulative percentage of the Desert on point B(\%))} \quad (2)$$

$$D_p = 1 - E_p - R_p \quad (3)$$

In this paper, the surface granularity data were imported by Matlab software and the end element analysis tool AnalySize1.1.2, and the Gen.Weibull method was selected for parametric end element analysis. The selection of end element

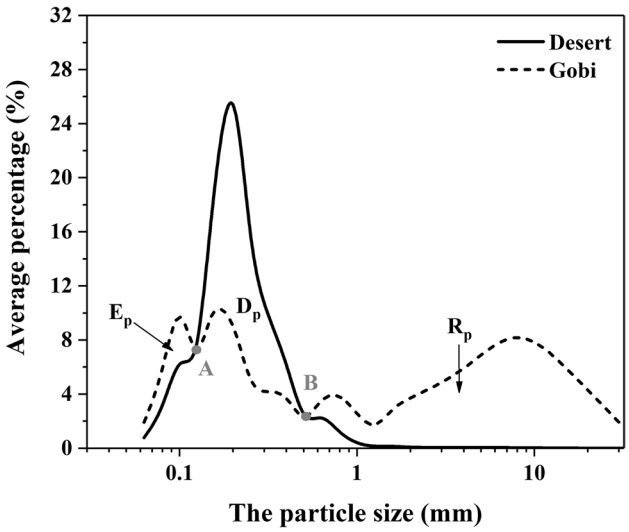

Fig. 3 Grain spectral profiles of surface sediments in the study area

number should consider the following indicators: (1) linear correlation (R^2), which represents the correlation between the original data set and the end element, the greater the value, the greater the correlation; (2) angle deviation, representing the end element and the original particle component curve in shape fitting, the larger the value indicates the greater the error of the end element curve in the shape fitting; and (3) end element correlation represents the correlation between each end element, and the greater the value

indicates the better the fitting degree. In general, when the linear correlation $R^2 > 0.8$, the angular deviation < 5° and the end element correlation is more small, the fitting degree is good, and when the above indicators are met, the least end element should be selected.

Sediment fractal dimension calculation and its variability

According to the dynamic characteristics of particle sand, the sediment components primarily included wind erosion particles (suspension and jump components) and sediment particles (creep and wind erosion residual components) and they had fractal characteristics. Accordingly, we applied the formulas to calculate the fractal dimension value of the Gobi surface sediment components (Liu et al. 2022). The specific formulas are shown in Eqs. (4) and (5):

$$D_i = 3 - \lg\left[\frac{w\left(\delta < \overline{d}_i\right)}{w_0}\right] / \lg\frac{\overline{d}_i}{\overline{d_{\max}}} \tag{4}$$

$$D = \sum_{t=1}^{n}\left(\frac{D_1^2 + D_2^2 + \cdots + D_n^2}{\sum D_i}\right., \tag{5}$$

where D is the fractal dimension of the soil particles; D_i is the fractal dimension value for each particle diameter segment; $\overline{d}_i$ is the average diameter of soil particles between two adjacent siers, grades $\overline{d}_i$ and d_{i+1}($\overline{d}_i > d_{i+1}$, i = 1,2,3, …); $\overline{d_{\max}}$ is the average diameter of the largest granular soil particle; $w(\delta < d_i)$ is the accumulated weight of soil particle diameter less than $\overline{d}_i$; δ is a size; the w_0 is the total weight of all granular particles; n is the total number of particle sizes.

Variation function is the main method to describe the characteristics of regionalization variables. The theoretical calculation formula is as follows:

$$\gamma(h) = \frac{1}{2N(h)}\sum_{t=1}^{n(h)}\left[Z(X_i) - Z(X_i + h)\right]^2, \tag{6}$$

where $\gamma(h)$ is the average half variance of all point pairs with lag level h; $N(h)$ is the number of discrete point pairs with the same interval of h in space; and property values of $Z(X_i)$ and $Z(X_i + h)$ points X_i and h are observation points apart from X_i (Shi and Li 2006).

The nugget variance (C_0), structural variance sill (C_0+C), and the variation range (A) are important parameters for variation analysis. The nugget variance reflects the variability and measurement error of the variables at the minimum sampling scale. When the variation function increases with the delay distance, and it reaches a relatively stable constant, the curve is horizontal, and this constant is the structural variance sill. The ratio of C_0/C_0+C reflected the ratio of random variation to the total variation. When the ratio < 25%, the study system showed a strong spatial correlation between local and the whole when the ratio was from 25% to 75%; and when the ratio was > 75%, the local and overall correlation was weak. The Range means the interval distance of the sampling point when the value of the variation function reaches from the nugget variance to the structural variance sill. This value is the most important parameter of the semivariance function graph, which describes how the space-related differences vary with distance. In this variation range, the smaller the sample spacing, the greater the similarity and spatial correlation.

Wind condition data and drift potential calculation

We collected wind condition data from four weather stations in the study area (Baoyintu weather station, Bayinhure weather station, Baiyin chagan weather station, and Bayannuru weather station) using a Wind Sonic 2 d ultrasonic wind speed sensor. The wind speed measurement ranged from 0 to 60 m s^{-1}, resolution was 0.01 m s^{-1}, wind direction measurement range of 0°–359°, and resolution was 1°. The wind condition recording frequency was 1/600 Hz, the observation height was 10 m near the ground, and the data were collected from October 31, 2016, to June 14, 2020. The average wind speed and wind speed of 10 min from 2016 to 2020 to calculate the average wind speed, average sand wind speed, sand wind frequency, and DP in this area. According to relevant studies (Zhang et al. 2015), the starting wind speed was set to 5.0 m s^{-1}, and characteristic values, such as DP and average sand starting wind speed and frequency, were calculated. The calculation equation is as follows:

$$\mathrm{DP} = V^2\left(V - V_t\right)t, \tag{7}$$

where DP is drift potential, vector unit (VU); V is the starting sand wind speed and starting wind speed at the height of V_t of 10 m, unit (section); and t is the sandstorm duration, which was calculated by the sandstorm frequency. According to the standard meteorological station of China Meteorological Administration, the height of wind speed was 10 m, while the meteorological station in the study area determines the height of 5 m. Therefore, the wind speed conversion (Feng et al. 2022), and the calculation equation was

$$U_{10} = \frac{U_5\left(\ln 10 - \ln Z_0\right)}{\ln 5 - \ln Z_0}, \tag{8}$$

where U_{10} is wind speed of 10 m; U_5 is wind speed of 5 m, Z_0 is surface roughness, generally Z_0 = 0.01–0.2. According to the vector synthesis method, we combined the DPs of 16 directions to obtain the resultant drift potential (RDP) and

resultant drift direction (*RDD*), which reflected the size of the region's net sediment capacity. The ratio of resultant drift potential and drift potential was the directional variation index (*RDP*/*DP*), which was used to reflect the combination of wind direction in a region.

We divided the wind-energy environment according to the Fryberger method (Fryberger and Dean 1979), as follows: high energy (DP > 400 VU), medium energy (*DP* 200–400 VU), and low energy (*DP* < 200 VU). We divided directional variation index into the following three levels: high variation rate, corresponding to complex wind condition (≤ 0.3); medium variation rate, corresponding to blunt bimodal or sharp bimodal wind condition (0.3–0.8); and low variation rate, with single wind direction (> 0.8).

Results

Characteristics of sediment particle spectrum changes

The particle spectral characteristics of dunes and Gobi desert surface sediments in the study area are shown in Fig. 4 and Table 2.The coarse particle size gradually decreased in the order of Haili, Boketai, Yamaleike, and Baiyinchagan Deserts, at 0.620, 0.586, 0.524, and 0.351 mm, respectively. This result showed that the desert area carried strong sand wind and that the maximum wind speed weakened significantly. Compared with the fine particle content around the dune fields, which was less than 0.125 mm and the potential of surface wind erosion dust release, the content of fine particles in Boketai Desert, Yamaleike Desert, and the Gobi around the Haili Desert was higher by 25%, 24.02%, and 26.61%, respectively. The Boketai Desert, Yamaleike Desert fine dust release potential was significantly weaker than the Haili Desert, and the potential dust release rates were 6.98%, 6.13%, and 16.62%, respectively. The Haili Desert wind erosion suspension particle size was 0.137 mm, and the other desert area suspension particles were 0.125 mm, which further showed that the Haili Desert's local maximum wind speed was larger. The overall regional wind power was stronger than that the Boketai and Yamaleike Deserts. The content of fine particles on the surface of Baiyinchagan Gobi desert was low, 22.75%, but the potential wind erosion dust release rate was high, 10.71%. The results showed that he region had few wind events and the maximum wind speed

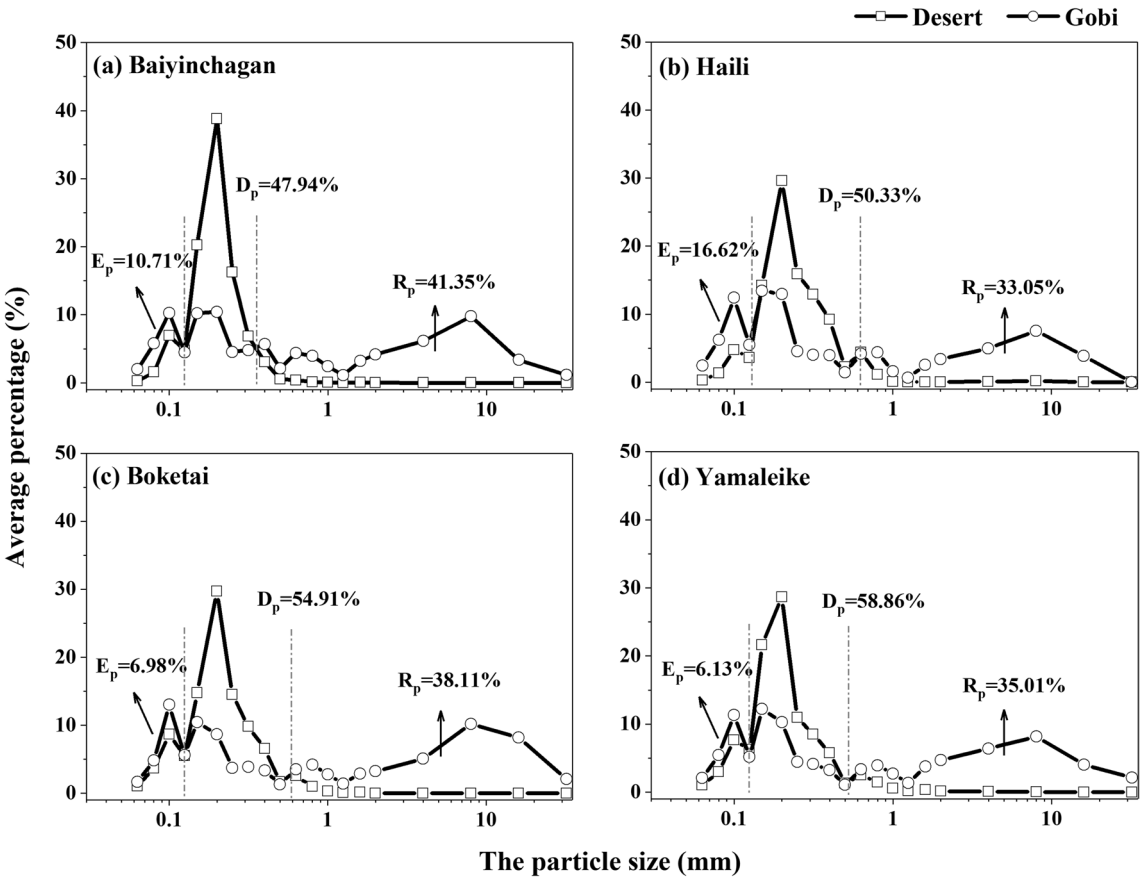

Fig. 4 Sediment particle profile characteristic curve

Table 2 Characteristics of the sediment component content

Surface	Location	The percentage of particles (%)					
		Micro sand	Silver sand	Medium sand	Coarse sand	Very thick sand	Gravel
		0–0.125 mm	0.125–0.315 mm	0.315–0.63 mm	0.63–1.25 mm	1.25–4 mm	4–32 mm
Desert	Baiyinchagan	3.391	20.542	1.34	0.792	0.02	0
	Haili	2.498	18.166	5.275	3.192	0.043	0.05
	Boketai	4.709	17.21	3.589	2.254	0.045	0
	Yamaleike	4.471	17.437	3.185	2.137	0.188	0.009
Average value		3.767	18.339	3.347	2.094	0.074	0.015
Gobi	Baiyinchagan	5.631	7.499	4.064	3.393	4.506	4.757
	Haili	6.652	8.734	3.184	2.766	3.622	3.849
	Boketai	6.274	6.671	2.724	2.756	3.734	6.816
	Yamaleike	6.004	7.773	2.565	2.609	4.956	4.775
Average value		6.140	7.669	3.134	2.881	4.205	5.049

of sand wind was affected by vegetation; however, low wind energy and dust events in the region were frequent, and the potential of dust release in the Gobi surface was large. Based on the particle size parameters of each desert sediment, we found that the characteristics of the source environment and the wind formation process of the surface were highly consistent from the perspective of energy.

The particle size parameters of desert dunes and Gobi desert surface sediments are shown in Fig. 5. The average particle size distribution of the four desert dune belts surface sediments was relatively concentrated and was distributed within the range of 0.05–0.5 mm, and the components. The sorting coefficient was distributed in the range of 0.02–0.3, and the sorting ability was moderate. Most of the sediment skewness showed extreme positive bias, and the peak states showed moderate broad flattening. The average particle size and sorting coefficient of the Gobi desert surface sediments showed a significant positive correlation linear relationship. The larger the average particle size, the worse the sorting, the distribution range of the average sediment particle size was wide (0–6 mm); the component was coarse; and the sorting coefficient was also wide (0–8). According to Fig. 5, the other three Gobi desert surface sediments featured extremely positive deviation, and the peak state featured.

Sediment granularity end members characteristics in west of Yinshan Mountain

In this paper, the end element analysis model is used to further reveal the environmental information and source of sediment. Considering the linear correlation, angular deviation and end elements correlations, the particle size data of the desert to the west of Yinshan and the surrounding Gobi sediment were decomposed into 3–5 end elements, and the fitting characteristics and results are shown in Table 3 and Fig. 6. As can be seen from the end-member frequency distribution curves, the desert end members showed a unimodal morphology, Population was near a normal distribution. Except the Boketai Desert, the main peak of EM1 in other desert were about 0.2 mm, indicating that EM1 is mainly composed of fine sand, while the main peak of EM1 in Boketai Desert was 0.1 mm, indicating that this EM1 component is composed of microsand; except the Haili Desert, the large particle size of EM2 and EM3, 0.35 mm and 0.6 mm, respectively, mainly with medium sand, EM2 and EM3 in other desert were 0.2 mm and 0.3 mm, still with fine sand. The surrounding Gobi end members showed multimodal morphology, indicating that the composition of the surface sediment is more complex. The main peak of EM1 was similar to desert, mainly composed of fine sand; the particle size for main peak of other end elements was gradually increased, mainly composed of coarse sand and gravel components, and the secondary peaks were small, indicating that the terminal component is also composed of some fine particle components except coarse particles.

Characteristics of the spatial distribution of sediment components and fractal dimensions

Figure 7 shows the spatial distribution diagram of dunes and Gobi desert surface sediment components (< 0.063, 0.063–0.5, and 0.5–32 mm) and fractal dimension. As shown in the figure, the suspension component of the dunes surface sediment was distributed mainly in the west of the Haili Desert and the south of the Yamaleike Desert, whereas the Gobi desert surface sediment suspension component was distributed mainly around the Haili and the Baiyinchagan Deserts. The content of the four desert surface sediment jump components was high, and the content of the four Gobi desert surface sediment jump

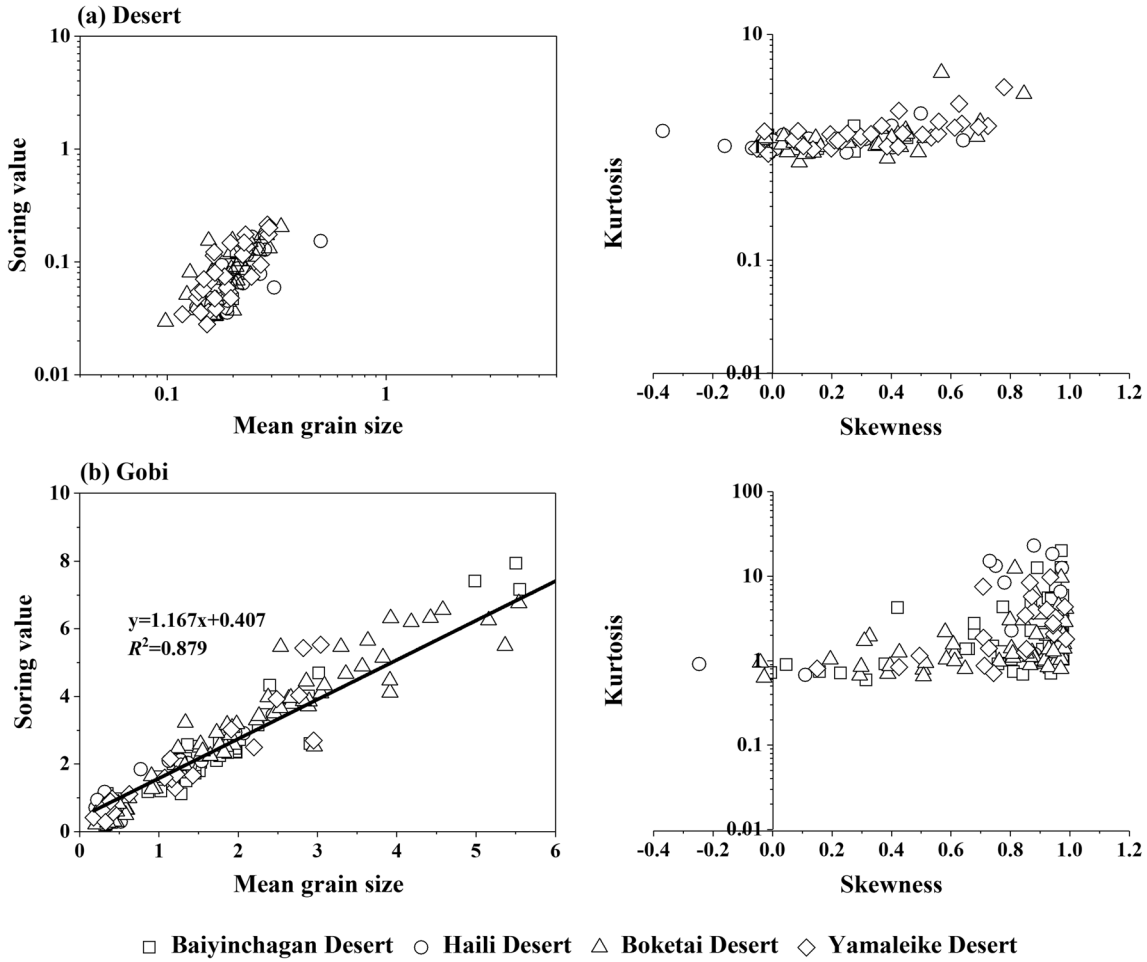

Fig. 5 Characteristics of the sediment particle size parameters

Table 3 End member fitting results

Surface	Number of end members	Linear correlations	Angular deviation	End members correlations
Baiyinchagan Desert	3	0.993	4.215	0.195
Haili Desert	3	0.902	16.255	1.840E-05
Boketai Desert	3	0.928	13.665	0.050
Yamaleike Desert	3	0.961	9.907	0.035
Baiyinchagan Gobi	5	0.884	13.702	0.019
Haili Gobi	4	0.899	13.515	0.180
Boketai Gobi	5	0.869	14.894	0.025
Yamaleike Gobi	4	0.862	14.981	0.034

components was in the middle. The content of creep and wind erosion residue was low, whereas the content of the four Gobi desert surface sediment was high, which was distributed in the west and north of Boketai Gobi. The spatial distribution of sediment components was closely related to the mountain distribution and wind trend in the study area, and was consistent with the characteristics of surface sediment components in dunes and Gobi desert. The maximum fractal dimension of dunes surface sediments was mainly distributed mainly in the west of the Haili Desert, in the east and south of the Yamleike Desert and in the north of the Baiyinchagan Desert, while the maximum fractal dimension of Gobi desert surface sediments was distributed around the Boketai Gobi, Haili

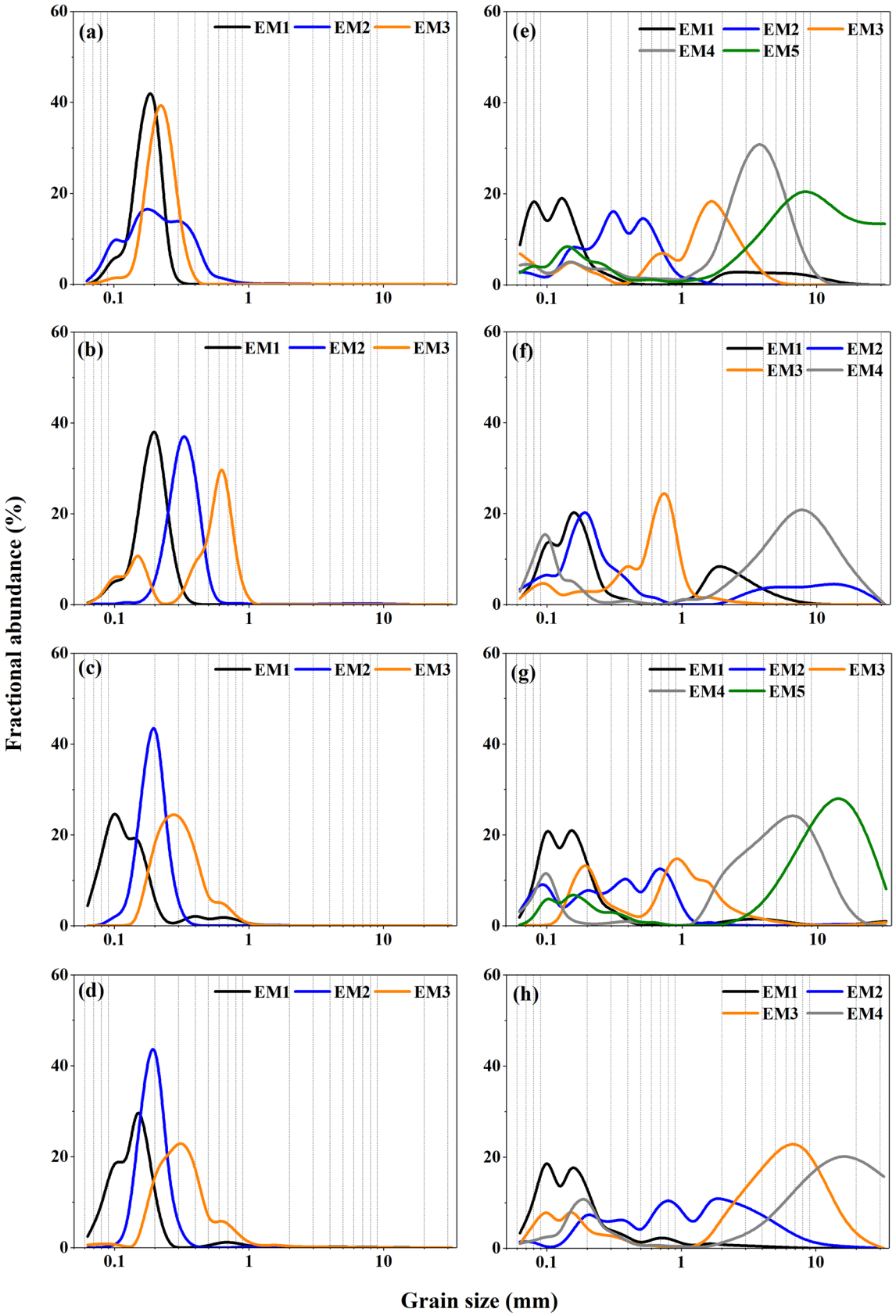

Fig. 6 End-member frequency distribution curves. **a** Baiyinchagan Desert; **b** Haili Desert; **c** Boketai Desert; **d** Yamaleike Desert; **e** Baiyinchagan Gobi; **f** Haili Gobi; **g** Boketai Gobi; **h** Yamaleike Gobi

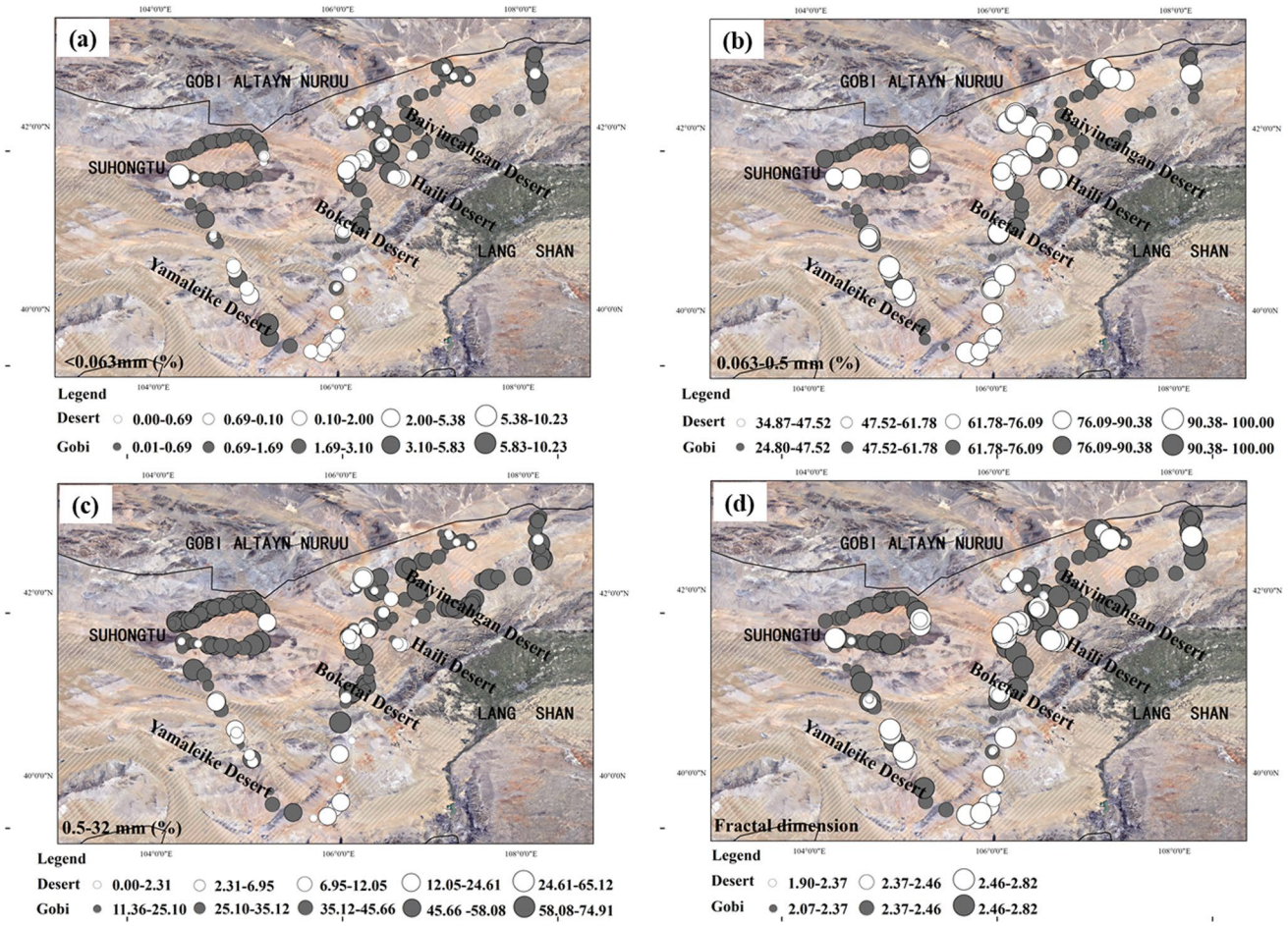

Fig. 7 Spatial distribution of sediment components and fractal dimensions

Gobi and Baiyinchagan Gobi. The spatial distribution characteristics of the fractal dimension were closely related to the sediment components, and the regularities of distribution were relatively consistent.

Characteristics of spatial variability in sediment particle size and fractal dimension

In this study, we compared the spatial variability of sediment components and fractal dimension of dunes and Gobi desert surface. As shown in Fig. 8 and Table 4, the spatial heterogeneity of sediment components and fractal dimension varied significantly, and the Gobi desert heterogeneity was significantly higher than that of the dunes surface. From the perspective of the three component heterogeneity, the suspension components of and jump component of the Gobi desert surface sediment were greater than that of the dunes surface, whereas the variation range of the creep component was smaller than that of the dunes surface. The ratio of nugget variance and structural variance sill showed that the suspension component of dunes surface sediment had moderate variability, whereas the jump component had strong variability, and the creep component did not have any spatial variation. Thus, the three components of Gobi desert surface all had moderate variability. From the perspective of fractal dimension heterogeneity, the fractal dimension variation of Gobi desert sediments was large, which indicated a large and moderate variation in space, whereas the dunes sediments are small and small in space, which indicated low variability.

Wind condition characteristics of the west desert of Yinshan Mountain

In this study, we used the wind speed data from the four weather stations in the study area (Baoyintu, Bayinhure,

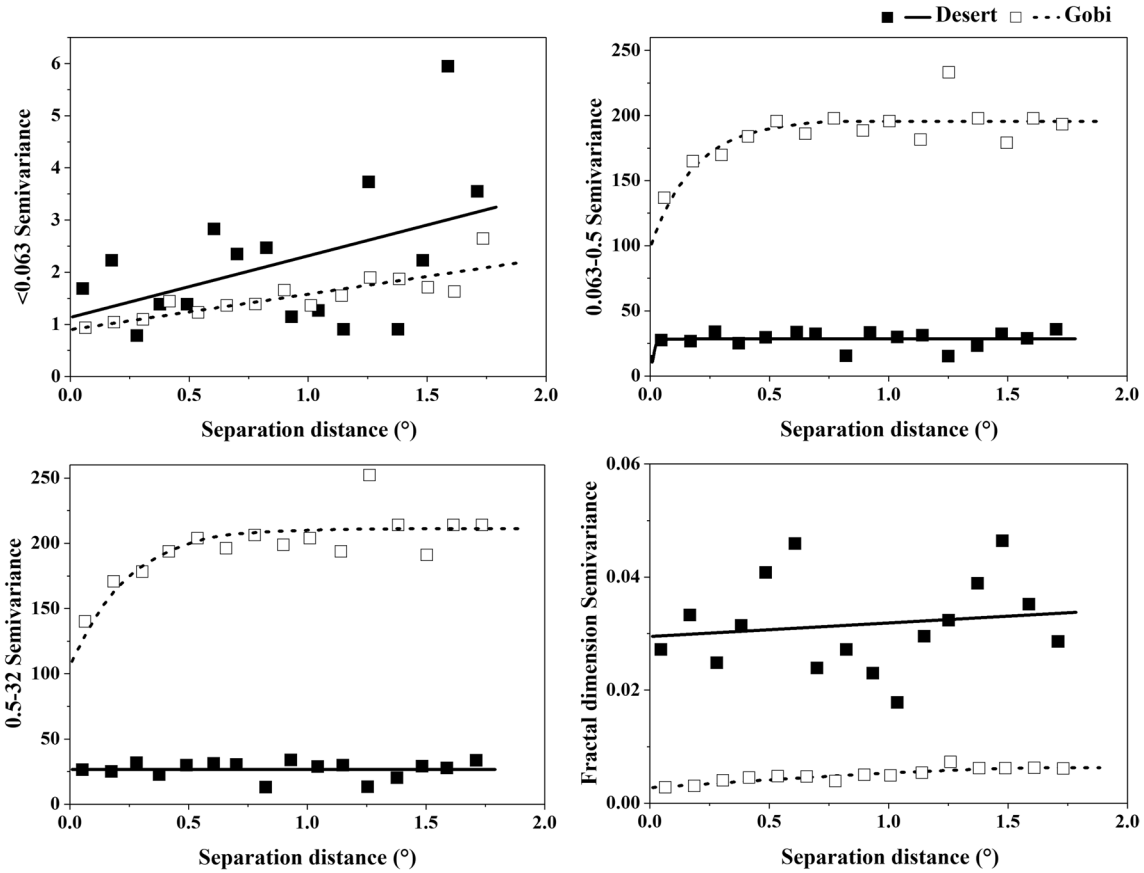

Fig. 8 Variation function curve of desert and Gobi surface components and fractal dimension

Table 4 Theoretical model of variation function by sediment component and fractal dimension

Surface	Variable	Model	Nugget variance	Structural variance sill	Range	Proportion/%	R^2	Residual SS
			C_0	C_0+C	°	$C_0/(C_0+C)$		
Desert	< 0.063 mm	Linear	1.122	3.178	1.712	35.310	0.214	21.8
	0.063–0.5 mm	Exponential	1.710	28.400	0.048	6.021	0.002	554
	0.5–32 mm	Linear	26.665	26.665	1.712	100.000	0.000	621
	Fractal dimension	Linear	0.029	0.034	1.712	87.340	0.026	9.634×10^{-4}
Gobi	< 0.063 mm	Linear	0.916	2.080	1.739	44.015	0.726	0.678
	0.063–0.5 mm	Exponential	98.100	196.300	0..546	49.975	0.649	2215
	0.5–32 mm	Exponential	105.400	210.900	0.681	49.976	0.679	2785
	Fractal dimension	Spherical	0.003	0.006	1.831	43.354	0.808	4.253×10^{-6}

Baiyinchagan, and Bayanuru) from 2016 to 2020. As shown in Fig. 9, the average wind speed and the average sand initiation wind speed in the study area in the past 5 years have fluctuated greatly. The annual average wind speed for the four stations (Baoyintu, Bayinhure, Baiyinchagan, and Bayanuru) from 2016 to 2020 was 5.13, 6.05, 5.42, and 6.08 m s^{-1}, respectively, and the annual average sand start wind speed in the area was significantly higher than the annual average wind speed, with speeds of 7.73, 8.87, 8.98, and 8.70 m s^{-1}, respectively. The frequency of sand wind in the north, east, south, and west of the study area increased first and then decreased from 2016 to 2020, indicating that the WSW are the dominant wind direction in this area, the frequency of sand breeze in 16 directions of

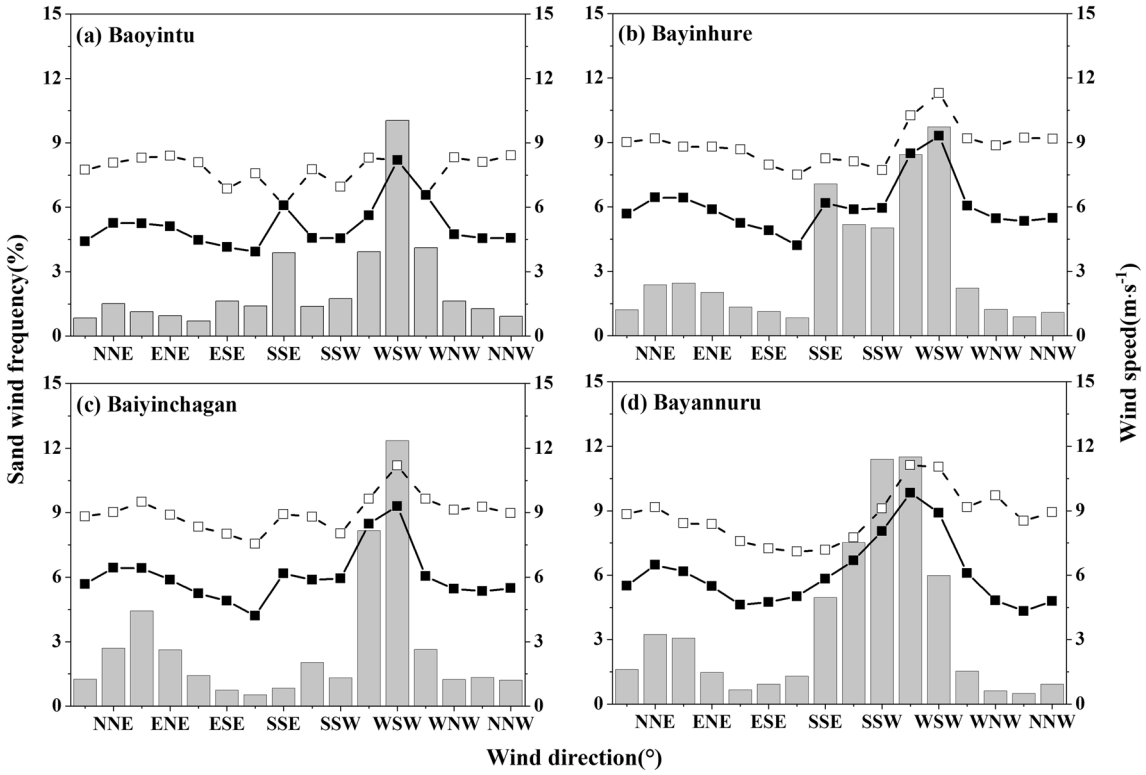

Fig. 9 Average annual wind speed, sand wind speed and sand wind frequency of the four weather stations in the research area from 2016 to 2020

the four meteorological stations was 3.93%, 8.43%, 8.16% and 11.50%, respectively. In general, in the past 5 years, the difference between the annual average wind speed and the annual average sand wind speed of the four weather stations was obvious, and the change characteristics of sand wind frequency were consistent with the characteristics of wind speed in this area.

DP is an important index used to measure the sandstorm activity intensity and wind dynamic environment in the area. The results calculated based on the wind speed data source in the study area are shown in Fig. 10. As shown in the figure, the average of the annual sediment DP from 2016 to 2020 was 359.99 VU, and the average of annual resultant DP was 204.46 VU, the sediment DP of the four weather stations is concentrated in the direction of southwest and west, and the difference in the direction of resultant DP is not large, namely, east–north–east and east–south–east close to the eastern direction. The average annual direction variation index was 0.55. The whole region exhibited a middle-wind-energy environment, middle-wind-direction variation, and blunt double-peak or sharp double-peak wind conditions.

Discussion

Grain size, fractal dimension, and their relationship

Because of the difference in wind energy environments, the grain size of Alxa Plateau desert sediment had a significant spatial difference. In the west desert of Yinshan Mountain, the dunes sediment was composed mainly of fine sand, with a mean grain size of 0.20 mm, and sorting value of 0.08. The sediment was coarse in Ulan Buh Desert, with a mean grain size of 0.14 mm, and a sorting value of 1.24, and the Kubuqi Desert, with a mean grain size 0.18 mm, and a sorting value of 0.57. The sediment was fine in the Tengger Desert, with a mean grain size 0.25 mm, and a sorting value of 1.02, and the Badain Jaran Desert, with a mean grain size 0.38 mm, and a sorting value of 0.62 (Song et al. 2016). The average particle size of the Gobi desert sediment in this area was 1.78 mm, in which the gravel component content of the area was high, which was related mainly to the mountainous and seasonal river sediments distributed around the study area. Thus, the particle size of the surface sediment was larger than that in the dune fields. On the whole, the internal particle size composition of the region has been refined from northwest to southeast and northeast, which was the result of the long-term dominant wind erosion integration.

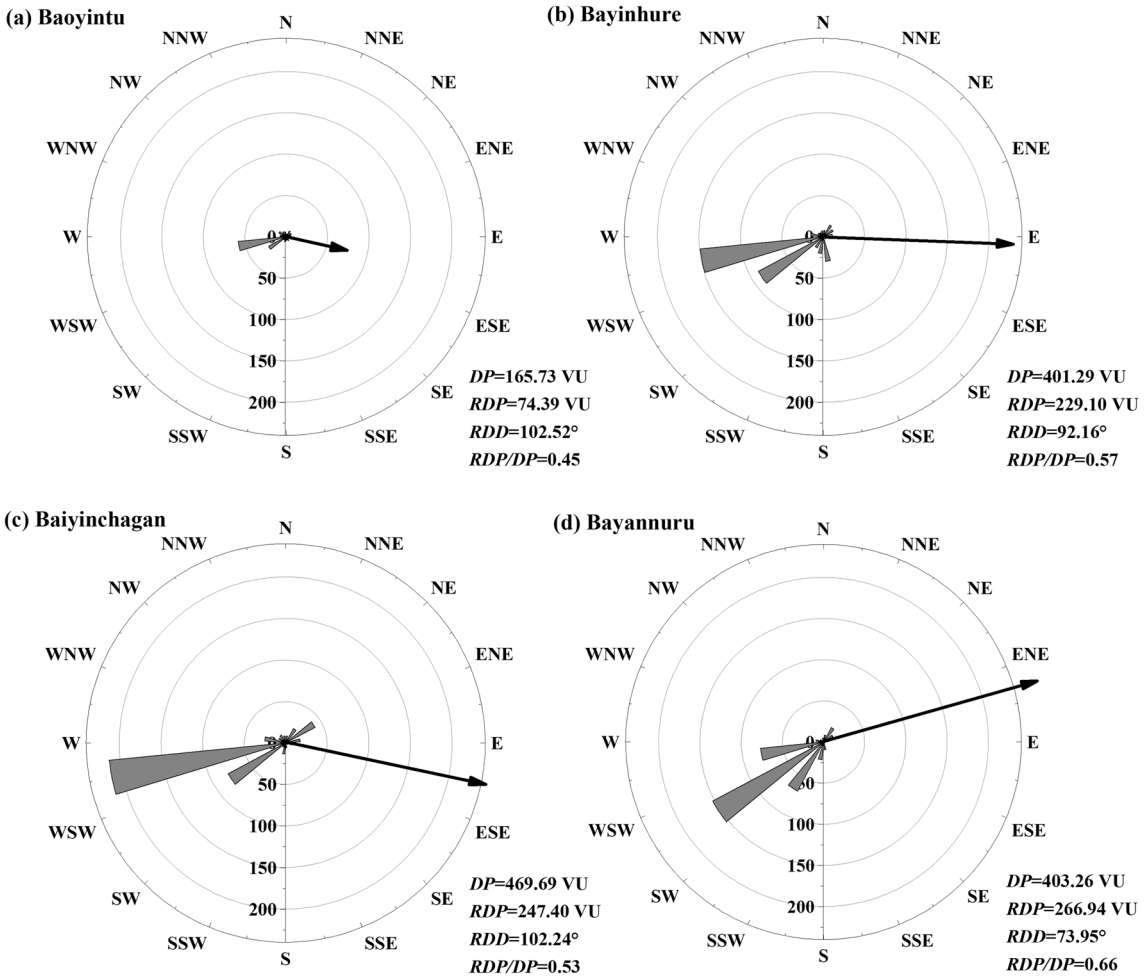

Fig. 10 Sand wind to transport sand potential rose map

The mean value of fractal dimension of dunes sediments in the western desert of Yinshan Mountain was 2.36, and the mean value of fractal dimension in Gobi desert was 2.43. The value of fractal dimension in the northern part of Boketai region and the southern part of Yamaleike region was large; The value of sediment fractal dimension in the north of Yamaleike Desert, east of Batai Desert, and west of Haili Desert was small, and the fractal dimension in the overall area gradually increases from northwest to southeast and northeast, which was consistent with the spatial differentiation law of sediment grain size. Strong hydraulic erosion effect, for instance, the particle size of river-flood sediment is large, fractal dimension value is between 2.80 and 2.86 (Wei and Hu 2014). Small main particle size of desert sand and loess matter under wind erosion, the fractal dimension is small, the value is 1.52–2.08 (Deng et al. 2017), and 2.12, respectively (Hou et al. 2021). The Gobi desert sediment formation process is more complex, early stage at the same time by wind and river two-phase erosion. In the later period, under the action of wind erosion, Gobi desert sediment particle size is coarse, the fractal dimension value is somewhere between desert sand and river-flood sediment.

Due to the complexity of soil system, some soil properties, such as soil particle surface characteristics, are difficult to quantify by conventional methods. The fractal dimension has practical significance for quantitative component proportional composition relationship and component type, In addition, this single parameter can indirectly reflect the influence of material transport on the distribution characteristics of the particle size of the desert surface sediment. As shown in Fig. 11, the components of the dune fields and Gobi desert surface sediment had a significant correlation with the fractal dimension. In this study, the distribution range of fractal dimension of desert sediment was 1.90–2.82, the average fractal dimension was 2.36, the distribution range of Gobi desert sediment was 2.07–2.59, and the average fractal value was 2.43. As shown in the figure, the fractal dimension of dunes surface and Gobi desert surface sediment were closely related to the components, especially the suspension component (< 0.063 mm) had a significant positive correlation.

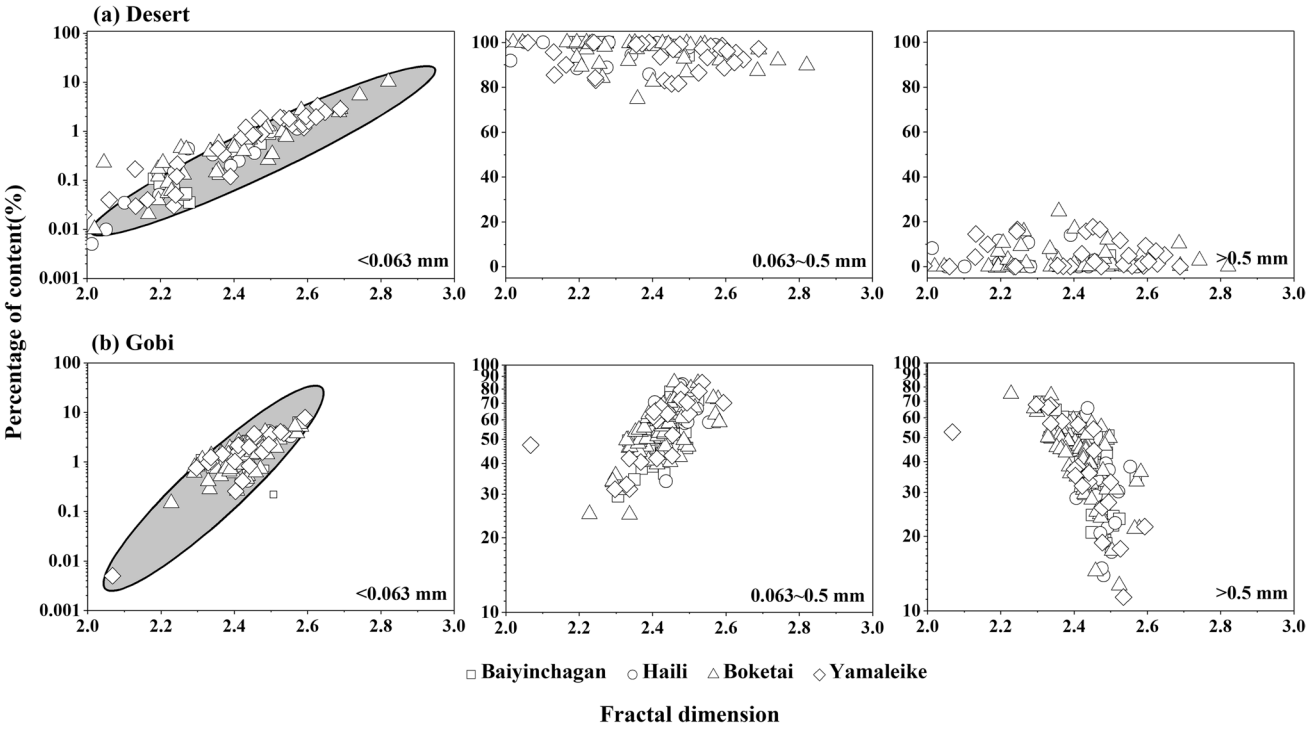

Fig. 11 Relationship between sediment components and fractal dimension

Thus, it was evident that the greater the content of easy wind erosion particles in the local surface sediment, the greater the fractal dimension value, and the higher the number of easily deposited particles, the smaller the fractal dimension value. The surface dust releases in arid areas and participates in the internal circulation process of dune fields and Gobi desert, which makes the regional surface sediments more heterogeneous, and the fractal dimension has reference significance when characterizing this surface process.

Sediment source and deposition process

Sediments record not only the information of wind transport alluvial process, but also the information of desert formation and development process and its sedimentary environment (Zhao 2001; Samuel and Akinade 2017). From the analysis results of the particle size end element model, the three end members were isolated from the desert sediments west of Yinshan, indicating that each end element indicates different deposition dynamic process and object source information. The end members of desert sediment was mainly microsand and fine sand, indicating that the sediment source in this area is mainly strong wind into sand transported by suspension or leaping; due to the strong wind force in several mountainous areas in the study area, the dry denudation hills and weathered erosion provided a rich sand source, the end component of Gobi desert sediment distributed in the desert downwind was more complex, mainly coarse sand and gravel, and some fine sand, and therefore, the source of such surface sediment included not only the sand sediments carried by the wind, but also the river and lake sediments, seasonal running water and the silt of rivers carried by the seasonal river flow.

In general, the sediment source and deposition process of the dune fields in west desert of Yinshan Mountain and the Gobi desert sediment has been affected by the sorting and sedimentation of debris sediment in the process of river and flood. Frequent dust internal circulation processes also have occurred between the dune fields and Gobi desert in this area (Wang et al. 2011), which have caused the surface material sedimentary environment to be significantly different.

Factors of sediment spatial differentiation

Many studies have demonstrated that dune fields in arid and semi-arid regions typically form part of local to regional scale sand transport systems, which comprise source areas, transport pathways, and depositional sinks. The dynamics of these systems are controlled by the supply of sand-sized sediment, the availability of this sediment for transport by the wind, and the transport capacity of the wind (Lancaster et al.2015, Lancaster and McCarley-Holder 2013). Therefore, wind condition, geomorphic pattern and source of sediments are the main factors influencing spatial differences of the dune surface sediment in the research area.

Under the action of wind, surface deposits are easily eroded, transported and deposited (Wang et al. 2021; Yang et al. 2004). The study area featured a low-wind-energy environment, the dominant wind direction is west–southwest, the annual average wind speed was 5.13–6.08 m s^{-1}, and the annual sand wind frequency was high. Under the action of the dominant wind, the gravel and residual coarse particle components on the surface of the original dust were transported and deposited in proximity. As a result, the nautical Haili Desert in the dominant wind direction was coarse, with large particle size and small fractal dimension value; and part of the fine particles material continued to participate in the subsequent sand transmission process, part of the release in the air, and part of the long distance transport and settlement. Thus, the original dust source on the surface of the fine particle composition content was reduced, making the dominant wind downwind Baiyinchagan Desert dunes and Gobi desert sediment component have a small particle size and low fractal dimension value. This area, however, still contained a small amount of fine particles, which mainly was due to the continuous collision and friction fragmentation between coarse particles under the action of sand in the process of sand transport, resulting in significant differences in the sediments in different areas.

Regional geomorphological pattern also had a certain influence on the surface spatial differentiation characteristics. Influenced by the distribution of obstacles, such as mountains in the study area, the sand-carrying capacity of carrying sand wind either increased or decreased (Chen et al. 2017; Cheng et al. 2022). For example, because of the influence of Agate Mountain, shelf Mountain, eastern Lang Mountain and its remaining veins in the study area, the wind speed with sand wind improved significantly, the kinetic energy of particle transportation increased, and the handling capacity of wind and sand flow also was significantly enhanced. Therefore, the sediment component of Haili Desert was coarse, and the fractal dimension value was small. In addition, the material into the sand flow changed the composition and content of the original sand sediment, which easily caused remote erosion. By contrast, the research area was mostly distributed in dune fields, Gobi desert, dry lake bed, and other dust released on the surface, mountain, and denudation hills through long-term weathering and denudation to form a large amount of debris material that accumulated in the foothill belt. In the process of wind and flood, this debris was transferred to the dust and released. In the process of wind and sand movement, the dunes and Gobi desert substances supplied each other, and fine particle substances, such as microsand and fine sand, occurred frequently in the local circulation. As a result, the spatial variability of dunes sediment components and fractal dimension was lower than that of the Gobi desert surface. The Gobi desert surface sediments had flood flushing and silt products, and the nearby desert sediments also were carried by the sand flow. Thus, the surface components were complex, with significant differences and large spatial variability.

Conclusions

The west desert of Yinshan Mountain featured blunt double-peak or sharp double-peak wind conditions with a middle-wind-energy environment and middle-wind-direction variability. The sediment onset was dominated by wind in the west and southwest directions, the average annual DP was 359.99 VU, and the average annual resultant DP was 204.46 VU.

The grain size in the dominant wind path in both the Haili Desert and Yamaleike Desert was coarse, while the particle size of the airflow convergence zone in the Baiyinchagan Desert and Boketai Desert were fine. The middle-wind-direction variability and low-wind-energy environment, as well as a sufficient supply of near-source Gobi coarse sand components, have made the Haili Desert and Yamaleike Desert to form stable, large-scale crescent dunes and dune chains.

The terrain of low hilly basins, in long-term high wind energy environments, the frequent flood process, dust cycle process, marked the desert sediment for sand sediment, and desert peripheral Gobi sediment for the wind-water under the formation of wind accumulation and river alluvial, and the Gobi heterogeneity was significantly higher than the desert surface, a moderate spatial specificity. The topography of low mountains and hilly basins affect the process of near-surface sandstorms and the formation and evolution of sandstorm landforms.

Acknowledgements This work was supported by the National Natural Science Foundation of China (Grant numbers 42261002 and 41861001).

Author contributions Dear editor, the author Liu Xiya conducted field sampling and indoor experiments, and completed the data processing and analysis and paper writing process. Author Wang Haibing helped with the setting of the experimental scheme and the final revision of the paper, author Zuo Hejun helped with the revision of the paper, and author Liu Nana helped in the field and indoor experiments. In the subsequent paper guidance process, Hejun Zuo* provided the project and some data support, as well as a lot of opinions and revision work, which was of great help to this article. Therefore, I have already communicated with all the authors, and the corresponding author was changed to Zuo Hejun, and has been modified in line 14~18 in the marked manuscript. I hope the chief editor can understand it

Declarations

Competing interests The authors have not disclosed any competing interests.

References

Adam SP, Paul RB, Anders JN, Maarten AP, Andrea L (2009) Holocene paleostorms identified by particle size signatures in lake sediments from the northeastern United States. J Paleolimnol 43(1):29–49

Bullard JE, Harrison SP, Baddock MC, Drake N, Gill TE, McTainsh G, Sun YB (2011) Preferential dust sources: a geomorphological classification designed for use in global dust-cycle models. J Geophys Res 116(F4):F04034

Chen SY, Huang JP, Li JX (2017) Comparative study of sand initiation, transmission and settlement in the Taklimakan Desert and the Gobi dust. Sci Sin (terrae) 47(08):939–957

Cheng H, Jiang N, Zhang KD, Wu B, Zou XY, Zhao XM (2022) Dust emissions in the Beijing-Tianjin sandstorm source and their regional differentiation. Chin Sci Bull 68:1356–1366

Deng JF, Li JH, Deng G, Zhu HY, Zhang RH (2017) Fractal scaling of particle-size distribution and associations with soil properties of Mongolian pine plantations in the Mu Us Desert, China. Sci Rep 7(1):6742

Dong ZB, Lv P (2020) Development of aeolian geomorphology in China in the past 70 years. Acta Geogr Sin 75(3):509–527

El-Baz F, Hassan M (1986) Physics of Desertification. Springer, Dordrecht, Netherlands

Feng JX, Ding ZL, You L, Han G (2022) Wind regimes and drift potentials in the corridor of transverse dunefield in western Korqin Sandy Land. J Desert Res 42(04):110–119

Folk RL, Ward WC (1957) Brazos river bar:a study in the significance of grain size parameters[J]. J Sediment Petrol 27(1):3–26

Fryberger, S.G., Dean, G., 1979. Dune Forms and Wind Regime[M]// Mckee E D.A Study of Global Sand Sea. Ashington, USA:US Geological Survey 137–172.

Hossein B, Mostafa R, Moharram MZ, Harry V (2015) Particle size distribution models, their characteristics and fitting capability. J Hydrol 529(3):872–889

Hou K, Qian H, Zhang YT, Zhang QY, Qu WG (2021) New insights into loess formation on the southern margin of the Chinese Loess Plateau. CATENA 204:105444

Kermani S, Boutiba M (2023) Grain-size analysis and quartz surface microtextures observations of sediments from Jijelian East coast, Algeria: sedimentary environment implications. J Sediment Environ 8(2):193–208

Lancaster N, McCarley-Holder G (2013) Decadal-scale evolution of a small dune field: Keeler Dunes, California 1944–2010. Geomorphology 180–181:281–291

Lancaster N, Baker S, Bacon S, Holder G (2015) Owens Lake dune fields: Composition, sources of sand, and transport pathways. CATENA 134:1–9

Li Y, Huang CM, Wang BL, Tian XF, Liu JJ (2017) A unified expression for grain size distribution of soils. Geoderma 288:105–119

Li JY, Gao XM, Dong ZB (2021) The dataset of wind regime for yardang landforms in the Qaidam Basin. J Desert Res 41(06):265–268

Li ZZ, Jin JH, Liu R, Xie XM, Zou XJ, Ma YQ, Tan DJ (2022) Review and prospect of aeolian geomorphology research in Gurbantunggut Desert, China. J Desert Res 42(01):41–47

Liu XY, Wang HB, Zuo HJ, Yan M, Li K (2022) Fractal of the Gobi surface sediment components and its variability characteristics. CATENA 218:106525

Lu S, Tang HM, Zhang YQ, Gong WP, Wang LQ (2018) Effects of the particle-size distribution on the micro and macro behavior of soils: fractal dimension as an indicator of the spatial variability of a slip zone in a landslide. Bull Eng Geol Environ 77(2):665–677

Mandelbrodt BB (1998) Fractal geometry of nature. Shanghai Far East Publishers, Shanghai, pp 8–11

Mohammadi M, Shabanpour M, Mohammadi MH, Davatgar N (2019) Characterizing spatial variability of soil textural fractions and fractal parameters derived from particle size distributions. Pedosphere 29(02):224–234

Nicholas PW, Craig LS (2011) Soil erodibility dynamics and its representation for wind erosion and dust emission models. Aeol Res 3:165–179

Paterson GA, Heslop D (2015) New methods for unmixing sediment grain size data. Geochem Geophys Geosyst 16(12):4494–4506

Porter SC, An ZS (1995) Correlation between climate events in the North Atlantic and China during the last glaciation. Nature 375(6529):305–308

Samuel O, Akinade O (2017) Depositional environments signatures, maturity and source weathering of Niger Delta sediments from an oil well in southeastern Delta State, Nigeria. Eurasian J Soil Sci 6(3):259–274

San José Martínez F, Martín MA, Caniego FJ, Tuller M, Guber A, Pachepsky Y, García-Gutiérrez C (2010) Multifractal analysis of discretized X-ray CT images for the characterization of soil macropore structures. Geoderma 156(1):32–42

Shen YP, Zhang CL, Wang DR, Wang XS, Cen SB, Li Q (2020) Spatial heterogeneity of surface sediment grain size and Aeolian activity in the Gobi desert region of northwest China. CATENA 188(C):104469

Shi Z, Li Y (2006) Application of geostatistics in soil science. China Agricultural Publishing House, Beijing, pp 3–9

Song J, Chun X, Bai XM, Si QBLG (2016) Review of grain size analysis in China Desert. J Desert Res 36(03):597–603

Su LD (2020) Analysis on the dynamic changes of desertification in Ulat Houqi from 1986 to 2019. Inner Mongolia Agricultural University, Berlin

Udden JA (1898) The merchaninal composition of wind deposits. Augustana Library Publications, Illinois, 3(1): 1–69

Wang XM, Zhang CX, Wang HT, Qian GQ, Luo WY, Lu JF, Wang L (2011) The significance of Gobi desert surfaces for dust emissions in China: an experimental study. Environ Earth Sci 64:1039–1050

Wang XM, Liang LL, Hua T, Zhang CX, Xia DS (2015) Geochemical and magnetic characteristics of aeolian transported materials under different near-surface wind fields: an experimental study. Geomorphology 239:106–113

Wang HB, Zuo HJ, Jia XP, Li K, Yan M (2021) Full particle size distribution characteristics of land surface sediment and their effect on wind erosion resistance in arid and semiarid regions of Northwest China. Geomorphology 372(1):107458

Wei L, Hu KH (2014) Study on sediment transporting characteristics of intermittent debris flows in Jiangjia Ravine. J Nat Disasters 23(02):53–60

Weltje GJ (1997) End-member modeling of compositional data: numerical-statistical algorithms for solving the explicit mixing problem. Math Geol 29(4):503–549

Xu QQ, Xiong KN, Chi YL (2021) Effects of intercropping on fractal dimension and physicochemical properties of Soil in Karst Areas. Forests 12(10):1422–1422

Yang XP, Rost KT, Lehmkuhl F, Zhu ZD, Dodson J (2004) The evolution of dry lands in northern China and in the Republic of Mongolia since the Last Glacial Maximum. Quatern Int 118–119:69–85

Young KP, Sung HP (2010) Development of a new wind-blown-dust emission module using comparative assessment of existing dust models. Part Sci Technol 28:267–286

Zhang ZC, Dong ZB, Qian GQ, Luo WY (2012) Wind energy environments and aeolian geomorphology in the western and South-Western Tengger Desert. J Desert Res 32(06):1528–1533

Zhang KC, Niu QH, An ZS, Zhang WM, Zhang H (2015) Aeolian dynamics environment near earth surface in Desert-Oasis

Transitional Zone of Dunhuang Area. Bull Soil Water Conserv 35(04):8–11+17
Zhang ZC, Pan KJ, Liang AM, Dong ZB, Li XC (2019) Progress on process and mechanism of sand and dust emission on Gobi. Adv Earth Sci 34(09):891–900
Zhao CL (2001) Sedimentary petrology. Petroleum Industry Press, Beijing, pp 48–72 (**253-260**)
Zhao WC, Liu LW, Chen J, Ji JF (2019) Geochemical characterization of major elements in desert sediments and implications for the Chinese loess source. Sci China Earth Sci 62(9):1428–1440
Zhou N, Li Q, Zhang CL, Hua HC, Wu YP, Zhu BQ, Cen SB, Huang XQ (2021) Grain size characteristics of aeolian sands and their implications for the aeolian dynamics of dunefields within a river valley on the southern Tibet Plateau: a case study from the Yarlung Zangbo river valley. CATENA 196:104794
Zhu ZD, Wu Z, Liu S (1974) Introduction to the desert in China. Science press, Beijing